IJES *Iranian Journal of Earth Sciences*
Vol. 13, No. 1, 2021, 50-58.

Rapid moment magnitude estimation for large earthquakes in Iran using time integration of absolute ground accelerations

Hossein Sadeghi*[1], Behnam Rahimi[1], Parvin Babaei[2]

1. Department of Geology, Faculty of Science, Ferdowsi University of Mashhad, Mashhad, Iran
2. Earthquake Research Center, Ferdowsi University of Mashhad, Mashhad, Iran

Received 25 May 2019; accepted 14 May 2020

Abstract

A total of 324 strong ground-motion records from 26 earthquakes with moment magnitude greater than 6 were used to derive an adequate equation for moment magnitude estimation. A parameter called total effective shaking was used to introduce an empirical equation for determining the near real-time magnitude of the Iranian plateau. This parameter was obtained through time integration of the absolute acceleration values from accelerograms over the strong shaking duration. It can be calculated by a simple mathematical procedure 5 seconds after completion of the waveform by decreasing the amplitudes to less than 20% of the maximum ground acceleration. The total effective shaking has a dimension of velocity and corresponds to moment magnitude and hypocentral distance in an attenuation relationship. The optimum coefficients were calculated through least-square regression analysis. Also, the effect of site conditions was evaluated in the analysis. The average shear-wave velocity to a depth of 30 m beneath each recording station was taken into account as the local site effect for 147 records out of the total number of records. The estimated moment magnitudes are in reasonably good agreement with the Global CMT values. Their differences are mostly less than 0.25 in the magnitude unit.
Keywords: *Earthquake, Magnitude, Early warning, Strong motions, Seismic attenuation.*

1. Introduction

Advances in the technology of manufacturing seismic equipment and communication links allow application of real-time earthquake information systems. Utilization of real-time systems, reduce casualties and damages significantly following a large earthquake. For assessing the losses in damaged areas, these systems estimate the main parameters of earthquakes such as time, location, and magnitude (Kanamori et al. 1997). A fast estimate of reliable earthquake magnitude in a short time after an event occurrence is essential to produce ground shaking and damage distribution maps in rapid response systems. Iranian plateau is located in the extensive Alpine-Himalayan orogenic system (e.g. Alavi 1994), which is the world's second major seismically active belt following the circum-Pacific belt, with 17% of the world's largest earthquakes (USGS 2020). Unlike other parts of the Alpine-Himalayan system, where active deformation is spread across regions several thousand kilometers wide, almost all the convergence is accommodated within the political borders of Iran itself (Walker and Jackson 2004). Engdahl et al. (2006) suggested that the vast majority of the earthquakes in Iran occur in the upper crust. Iran has experienced destructive earthquakes such as Tabas earthquake in 1978 with the magnitude of 7.3, Rudbar-Manjil earthquake in 1990 with the magnitude of 7.4, Zirkuh (Qa'enat) earthquake in 1997 with the magnitude of 7.2, Bam earthquake in 2003 with the magnitude of 6.6, and Sarpolzahab earthquake in 2017 with magnitude 7.4 (Global CMT catalog, www.globalcmt.org).

These events caused significant loss of life (e.g. Berberian 2014; Shahbazi and Mansouri 2019). The availability of a relatively extensive strong motion databank in Iran makes it possible to apply an accelerometric data-based method for rapid estimation of earthquake moment magnitude. Predicting the final size of a large earthquake from body wave magnitude is inherently difficult because the classical body wave magnitude saturates at about 6 (Lee et al. 2012). Also, obtaining the moment magnitude of a large earthquake by the classical method of spectrum of far-field body waves faces an inherent problem because it is difficult and almost impossible to distinguish the far-field P and S waves in near-field records (Delouis et al. 2009). On the other hand, waveform inversion methods generally take more than 10 minutes to measure the final size of a large earthquake (e.g., Lee et al. 2012). So, we decided to investigate and propose a method for more rapid estimation of moment magnitude for large earthquakes in the Iranian plateau by using strong motion data. The rapid magnitude estimation for early warning systems is usually based on the measurement of peak amplitude or dominant period within the first 4 seconds of the recorded P and S wave train (e.g., Allen and Kanamori 2003; Allen 2007; Wu and Kanamori 2008; Zollo et al. 2010). There are also methods based on the relation between released energy and earthquake magnitude (Wu and Teng 2004; Festa et al. 2008). Wu and Teng (2004) proposed that the released earthquake energy corresponds to a strong ground motion parameter called total effective shaking.

*Corresponding author.
E-mail address (es): sadeghi@um.ac.ir

They successfully applied this parameter to rapidly estimate the earthquake moment magnitude using the recorded data by Taiwan's strong motion network. This method utilizes a simple and straightforward mathematical procedure for the determination of earthquake magnitude with acceptable accuracy just after a waveform has been completed. The advantage of their approach is that it considers a significant part or nearly entire of the waveform for magnitude estimation. They discussed that due to rupture complexity in a large earthquake, we are not likely to get reliable magnitude information by using the first seconds of P-wave arrival. To improve the accuracy of the magnitude estimation by the early portion of the wave train, Colombelli et al. (2012) and Colombelli and Zollo (2015) suggest measurements of the dominant period over a progressive expanded P-wave time window. Based on the frequency content of acceleration parameters, some studies optimized the magnitude estimation for the earthquake early warning system around Tehran region (Heidari et al. 2013; Nazeri et al. 2017). However, estimating the magnitude of large earthquakes through the initial seconds of nucleation rupture (P-wave) is difficult and unreliable. This is because large events with large rupture suggest a number of strong asperities over the entire rupture volume. Therefore, for large crustal earthquakes recorded by nearby stations, a method relied on released energy such as Wu and Teng (2004), can be useful. The method introduced by Wu and Teng (2004) has been chosen for rapid estimation of moment Magnitude for M>6.0 earthquakes recorded at hypocentral distances up to 150 km. The proposed method works on waveform times series. The end-of-event times of the records used in their study are less than 2 minutes at an epicentral distance of less than 150 km. Therefore, the moment magnitude can be estimated within 2 minutes using an acceleration time series within 150 km of epicentral distances. The empirical method of Wu and Teng (2004) was employed by Lin and Wu (2012) for fast magnitude determinations of crustal earthquakes in Japan. They showed that this method can be applied in other regions, and can be appropriate for extremely large events such as the Great Tohoku Earthquake of 2011 (Mw 9.0) without a saturation problem.

2. Method

The method proposed by Wu and Teng (2004) has been employed. They introduced an empirical formula for rapid magnitude determination of shallow large earthquakes. They used strong ground-motion databank of Taiwan with moment magnitude 5.7 and greater and depth of less than 35 kilometers. In this method, a parameter, namely, total effective shaking, is defined which is corresponded to the energy released by an earthquake. The total effective shaking is an integral of absolute values of the acceleration over the duration of strong shaking as:

$$\sqrt{ES} = \int_{T_p}^{T_e} \sqrt{V^2 + N^2 + E^2}\, dt \qquad (1)$$

Where, V, N, and E are baseline corrected vertical, and north-south, and east-west components of accelerogram respectively. T_p is equivalent to the onset time of P wave, and T_e is the end of duration time for the event's strong shaking. T_e is defined as 5 seconds after the acceleration amplitude decreases to 20% of the maximum value of amplitude. Acceleration values are in cm/s^2 and the time unit is second. Fig 1 shows an example of the procedure for calculating the total effective shaking. Fig 1a is L (N330ºE) horizontal component of the acceleration record of the 1997 Zirkuh (Qa'enat) earthquake with magnitude of 7.2. The waveform was recorded at Sangan station with epicentral distance of 69 km. Fig 1b shows the absolute amplitude. The absolute amplitude decreases to 20 percent of the maximum amplitude at 62 seconds and preserves it for 5 seconds. So by integrating from P-wave onset time to the end of the 5 seconds preserved time, the value of total effective shaking, $\sqrt{ES}$, would be determined (Fig 1c). The obtained quantity is in the dimension of velocity so it would be corresponded to wave energy. Thus the method utilizes the relation between the wave energy and the event magnitude for rapid magnitude estimation.

All of the strong motion records used in this study are from the earthquakes with focal depth less than 30 kilometers. Since the Moho depth is, generally, deeper than 40 km beneath Iran (e.g., Asudeh 1982; Dehghani and Makris 1984; Nasiripour 2006), the selected events can be considered as the crustal earthquakes. Following Wu and Teng (2004), equation (2) was used for the attenuation relationship between $\sqrt{ES}$ and event moment magnitude:

$$\log(\sqrt{ES}) = A + B \cdot Mw + C \cdot R + D \cdot \log(R) + S_i \qquad (2)$$

Where Mw is moment magnitude, R is the hypocentral distance in km. S_i is the site correction factor for ith station and can be determined as the ground motion amplification due to the near surface soil properties. The values of coefficients A, B, C, and D were estimated by least square regression analysis.

3. Data

The databank of Iranian Strong Motion Network (ISMN) was used in this study (BHRC 2018a). ISMN has started its activity since 1973 with using Kinemetrics SMA-1 analog instruments. The SSA-2 digital accelerographs were installed after the 1990 Rudbar-Manjil earthquake, and newly installed instruments are Guralp CMG-5TD. The ISMN currently has more than 1100 operational accelerograph stations in Iran.

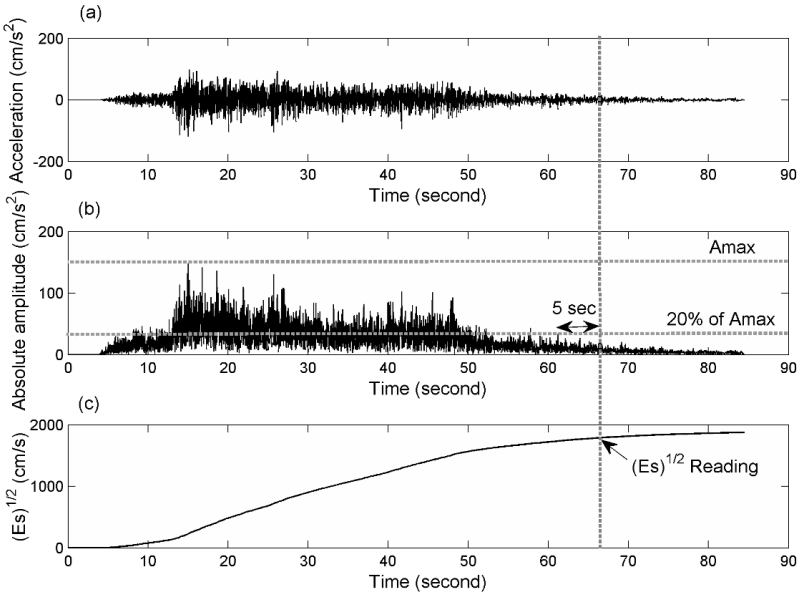

Fig 1. An example of the process used for calculating the total effective shaking parameter. (a) The waveform of the L (N330ºE) component of the May 10, 1997 Zirkuh (Qa'enat) earthquake (Mw 7.2) at Sangan station. (b) Time series of absolute amplitude considering all the three-component data. The upper and lower dashed lines indicate maximum amplitude and 20% of that, respectively. (c) Integrating of absolute amplitude and reading the value of the total effective shaking parameter.

More information on ISMN is available on the web page http://www.bhrc.ac.ir of the Building and Housing Research Center of Iran (BHRC). The data used consists of 324 strong motion records of 26 earthquakes with a moment magnitude of greater than 6, which occurred in the Iranian plateau from 1977 to 2017. Fig 2 shows the locations of epicenters of the earthquakes and the recording stations. Information on moment magnitude and epicentral location of the earthquakes were obtained from GCMT and USGS/NEIC catalogs, respectively. The values of the focal depths were compiled from Engdahl et al. (2008) and the catalog of the USGS/NEIC, respectively before and after the end of 2008. In Fig 3, the distribution of the records with respect to hypocentral distance and magnitude, are shown. The figure shows that the maximum hypocentral distance is 150 km and the distribution of magnitudes ranges between greater than 6 and less than 7.5, with a gap in the range of 6.7 to 7.1. There is a considerable number of records at short hypocentral distances (less than 50 km), but almost all of them correspond to earthquakes with magnitudes less than 6.7.

Along with source distance and earthquake magnitude, near-surface site condition is the other fundamental factor which affects the ground motion from an earthquake. The site amplification term is taken into account in Ground-Motion Prediction Equations (GMPEs) and has been supported by many literatures (Douglas 2019). Since the ground motion parameters are affected by recording site conditions, the stations in the study area were classified based on average shear wave velocity over the upper 30 m depth (Vs30). The Vs30 is a widely used parameter for site classification in many earthquake design codes such as NEHRP (1997), EUROCODE 8 (2004), and *Iranian standard code*; Standard 2800 (2014). The basic concept of the Vs30 comes from the fact that the near-surface shear wave velocity affects the site amplification (e.g. Borcherdt and Gibbs 1976).

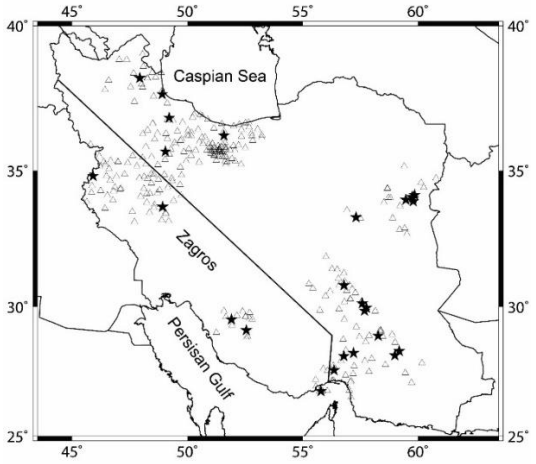

Fig 2. Locations of the 295 strong ground-motion stations (BHRC, https://smd.bhrc.ac.ir/), and the epicenters of 26 earthquakes (USGS/NEIC, https://earthquake.usgs.gov) with moment magnitude greater than 6 (GCMT, https://globalcmt.org) which were used in this study are shown by open triangles and solid stars, respectively. The line divides the stations into two regions: the Zagros region and the rest of Iran.

Many researches (e.g. Boore and Atkinson 2008; Borcherdt and Glassmoyer 1992; Midorikawa et al. 1994; Mase et al. 2018a; Mase et al. 2018b) have found a good correlation between the Vs30 and the amplification of ground motion. The Building and Housing Research Center of Iran (BHRC 2018b) has made the Vs30 available for 138 of the 295 stations used in this study. The number of strong motion recorded by these stations is 147 out of the total number of 324 records. Consequently, the site conditions of 47 percent of the stations (i.e. 100×138/295) and 45 percent of the records (i.e. 100×147/324) were defined.

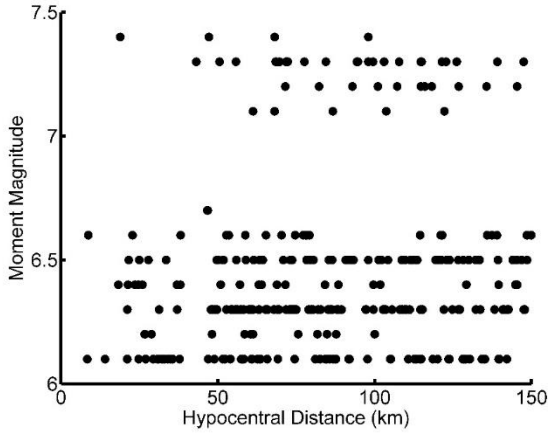

Fig 3. Distribution of the records with respect to moment magnitude and hypocentral distance.

4. Calculation Procedure and Results

The *least squares (lm) function in the* R statistical software (R Core Team 2020) was used to determine the coefficients in Equation 2. The regression Equation was first investigated considering the site correction term by the Vs30 parameter. The statistical analysis was limited to regression on 147 records which have the Vs30 information. *Iranian standard code*, Standard No. 2800 (2014), divides the sites into four classes according to the Vs30. The four classes are: Class I (Vs30 > 750 m/sec), Class II (375 <= Vs30 >= 750 m/sec), Class III (175<= Vs30 > 375 m/sec), Class IV (Vs30 < 175 m/sec). Since there are very few records with Class IV, the regression relationship was estimating by categorizing the data set into three classes (Class I, II, and III). We benefited the statistical technique of using dummy variables for obtaining site correction terms. The Application of dummy variables is one of the usual methods in the regression analysis for partitioning data to several separate sections (Weisberg 1980). The same application was also used by the previous studies on strong motion records for classification data (e.g., Joyner and Boore, 1981; Pankow and Pechmann, 2004). Therefore, the following model was considered:

$$\log(\sqrt{ES}) = A + B.Mw + C.R + D\log(R) + E.S_{II} + F.S_{III} \quad (3)$$

$S_{II} = 0, S_{III} = 0$ for Class I (rock site)
$S_{II} = 1, S_{III} = 0$ for Class II
$S_{II} = 0, S_{III} = 1$ for Class III

Where S_{II} and S_{III} are dummy variables. The coefficients of Equation (3) were determined by using the lm (multiple linear regression) function, and the correlations between the variables were determined by using the Pearson correlation analysis.

The results are depicted in Table 1. Based on the results represented in Table 1, the correlation and regression analysis indicate that R and $\log(R)$ are strongly correlated to each other and the p-value for the coefficient for the anelastic attenuation (C), is not statistically significantly different from zero because its p-value is definitely greater than 0.05. Thus, the variable R was removed from the next regression equations. Table 1 also indicates that the coefficient E for the dummy variable S_{II} is not statistically significant because its p-value (0.786) is much greater than the usual significant level of 0.05. This means that the data is not statistically suitable for using the dummy variables for site classification. Thus, the Vs30 values were directly used for the site correction term, and the regression equation was considered as follows:

$$\log(\sqrt{ES}) = A + B \cdot Mw + D \cdot \log(R) + E \cdot \mathrm{Vs30} \quad (4)$$

Here the unit used for Vs30 is km/sec. The regression results are presented in Table 3.

The multiple linear regression was also conducted without considering the site correction term and the coefficients were determined as the following equation;

$$\log(\sqrt{ES}) = A + B \cdot Mw + D \cdot \log(R) \quad (5)$$

The coefficients were determined using all the 324 records of Iran as a whole and the attenuation relationship for $\sqrt{ES}$ is given by:

$$\log(\sqrt{ES}) = 0.540 + 0.564\,Mw - 0.933\log(R) \quad (6)$$

The regression results are presented in Table 1. On the other hand, due to the difference between seismotectonic characteristics of various provinces in the Iranian plateau, the seismotectonic zonation was also considered in the model. There are detailed divisions for the seismotectonic structure of Iran (e.g., Takin 1972; Berberian 1976; Nowroozi 1976; Engdahl et al. 2006). However, the data is not sufficient for a detailed zonation. Only two regions: Zagros and the rest of Iran was considered. The stations divided into these two main regions for performing the regression analysis (Fig 2). This categorization was conducted in some previous studies on strong motion attenuation determination for Iran (e.g., Zare et al. 1999; Ghodrati et al. 2007, Saffari et al. 2017). The Zagros region has been separated from the other areas of Iran because of the frequent occurrence of the earthquakes along the Zagros belt and their smaller magnitude with respect to other regions.

Table 1. Correlation and regression analysis result for equation 3. The bold font shows a strong correlation between the two variables and a statistically insignificant coefficient (p-value > 0.05).

Pearson Correlations				Coefficients						
	Mw	R	Log(R)		A	B	C	D	E	F
Mw	1			Value	1.038	0.549	0.0018	-1.229	0.013	0.014
R	0.148	1		STD	0.479	0.055	0.002	0.250	0.049	0.064
Log (R)	0.150	**0.945**	1	p-value	0.032	0.000	**0.290**	0.000	**0.786**	0.030
				N=147 Residual (RMS)=0.245 R^2= 0.617						

N is the total number of data, STD is the standard deviation

Table 2. Regression analysis result for equation 4.

Coefficients				
	A	B	D	E
Value	0.842	0.552	-0.984	-0.156
STD	0.377	0.055	0.082	0.072
p-value	0.027	0.000	0.000	0.033
N=147 Residual (RMS)=0.245 R^2= 0.612				

N is the total number of data, STD is the standard deviation.

The regression analysis results, based on a total of 86 and 238 recordings respecticely for Zagros and the rest of Iran, are given in Table 3. This Table and also Table 2 show that the R^2 of the regression models are relatively low, but the coefficients are significant (p-value < 0.05) to explain the total effective shaking. Fig 4 shows the plot of the residuals of the regression equation 5 against the hypocentral distance for all of 324 data. The residuals scatter randomly around zero for the entire range of data. This combination of no systematic bias in the residuals and statistically significant independent variables suggest that the model made a perfect prediction, while due to relatively low R^2, precise predictions are not expected. In general, a low R^2 means that there are inherently more unexplained variations in the data, and adding variables to the model can improve R^2. The regression analysis results show an increase in R^2 for the model with data limited to the Zagros seismotectonic region (Table 3) and also the model with site effect term (Table 2), although this increase can depend on the number of data used (e.g., see Zaarour and Melachrinoudis 2019).

5. Discussions and Conclusions

This article attempted to derive an attenuation relationship for rapid determination of moment magnitude that is one of the fundamental parameters of the earthquake in near real-time studies, using strong motion data in Iran. The obtained result could be applied in rapid response systems after a large earthquake. The data used in this study were recorded by 295 stations of Iranian strong motion network over the period 1977-2017. The coefficients of the attenuation relationship introduced by Wu and Teng (2004) were estimated through a multiple linear least square regression according to the equation. (2). The site correction factor in the equation was determined by using the average shear-wave velocity over the upper 30 m (Vs30), which was available for 138 stations. The regression result for equation (4) indicates a higher level of the total effective shaking values on soil sites with lower Vs30. The most probable reason for this effect could be found in the fact that amplification on soil sites is more than on rock sites, so the released energy on soil sites is more than on rock sites. The regression coefficients were also obtained using the total data of Iran without considering the site correction term. With regards to existing of various seismic properties in different regions of Iran, we attempted to examine the feasibility of having different magnitude estimation equations for each region. Because of insufficient data for the regression analysis, a more general categorization for the seismotectonic of Iran: Zagros and the rest of Iran, was conducted. The attenuation curve for the whole of Iran is located between the Zagros and Iran except Zagros curves. However, the difference between a model based on data recorded across Iran and one based on no data in the Zagros region is negligible (Fig 5).

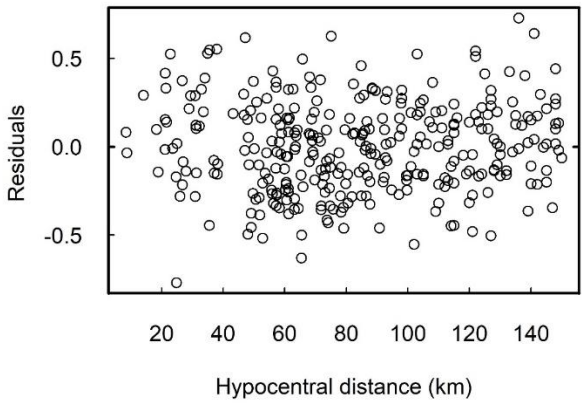

Fig 4. Distribution of residuals of the regression equation 5 against hypocentral distance for all of 324 acceleration records used.

Table 3. Regression analysis results for equation 5 for Iran and its two main seismotectonic regions, Zagros and Iran except Zagros.

Region	Whole Iran	Zagros	Iran except Zagros
Coefficients	A B D	A B D	A B D
Value	0.540 0.564 -0.933	1.287 0.499 -1.093	0.413 0.568 -0.882
STD	0.265 0.039 0.064	0.336 0.051 0.109	0.188 0.022 0.075
p-value	0.043 0.000 0.000	0.000 0.000 0.000	0.039 0.000 0.000
N*, Residual (RMS), R^2	324, 0.256, 0.525	86, 0.236 , 0.642	238, 0.259, 0.594

*N is the total number of data, STD is the standard deviation.

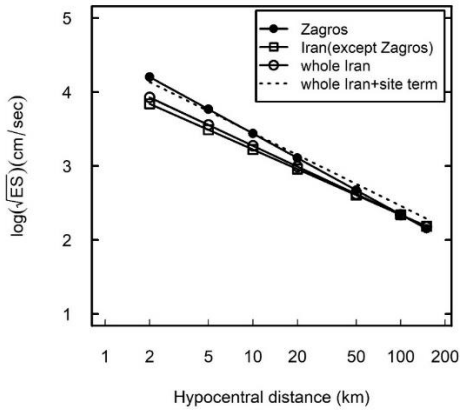

Fig 5. The comparison of obtained attenuation curves (Mw=6.5) for Zagros, Iran except Zagros, and whole Iran. Due to insufficient data recorded by stations containing Vs30 information, the regression model with the site correction term was conducted only for Iran as a whole.

It may be concluded that except for Zagros, there is no reliable basis for other seismotectonic classification based on the currently available data in Iran to the end of 2017. Fig 6 shows the comparisons between attenuation curves of this study and Wu and Teng (2004) for the 2006 Silakhor earthquake (Mw 6.1) in the Zagros region and the 2005 Zarand earthquake (Mw 6.4) outside the Zagros region in the southeast of Iran. The focal depths are based on the catalog of Engdahl et al. (2008). The differences of attenuation curves are related to short hypocentral distances and as the distance increases, the curves become closer to each other. For the Zagros model, the curves are merged after 100 km of hypocentral distance while this happens for the whole Iran and Iran except Zagros models after 20 km of hypocentral distance.

As the conclusion, by rewriting the equations (4) and (5), the following empirical equations are obtained for estimating moment magnitude (*Mew*) of the large crustal earthquakes in Iran, with and without considering site condition, respectively.

$$Mew = -1.524 + 1.812\log(\sqrt{ES}) + 1.7831\log(R) + 0.283Vs30 \quad (7)$$

$$Mew = -0.957 + 1.773\log(\sqrt{ES}) + 1.654\log(R) \quad (8)$$

The equations could estimate the moment magnitude soon after a waveform is completed. The total effective shaking, $\sqrt{ES}$, will be calculated just by integrating the absolute amplitude of the baseline-corrected acceleration time history, and the hypocentral distance, *R*, can be provided by a real-time location method (e.g., Kanamori, 1993; Sadeghi-Bagherabadi et al. 2013). Fig 7 shows the comparison between the reported moment magnitude and the estimated magnitude for all the events with 3 and more recordings. There is, in general, a good agreement between them.

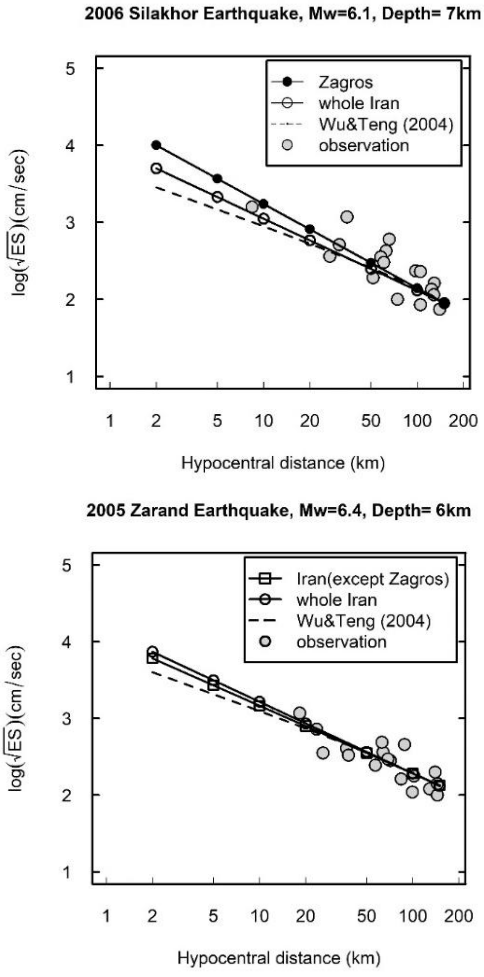

Fig 6. Attenuation curves for the total effective shaking, $\sqrt{ES}$, obtained by this study and by Wu and Teng (2004).

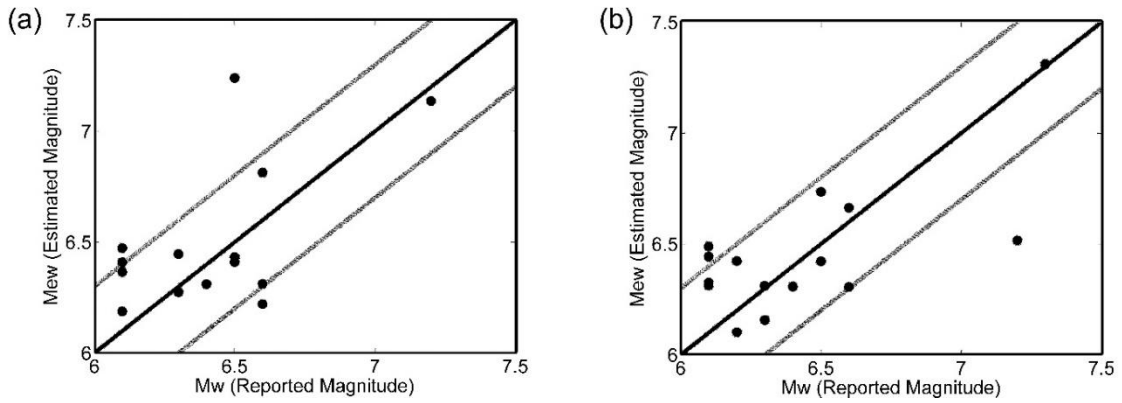

Fig 7. Comparison of reported (Mw) and estimated moment magnitude (Mew) of the earthquakes with three and more records. The black curve is a 45-degree line and gray curves are the black curve +/- 0.25 in the Mew axis. (a) regression without considering site condition, (b) regression considering site condition.

Acknowledgements

We are very grateful to the Building and Housing Research Centre, Iran for providing the strong-motion data. We sincerely thank Robert E. Engdahl for giving the hypocentral parameters of the events used in this study. We would like to thank Amir Sadeghi-Bagherabadi for his fruitful discussions and comments. The authors would also like to thank the three anonymous reviewers for their helpful comments that greatly improved the manuscript. Some figures in this paper were made using Generic Mapping Tools (Wessel and Smith 1998).

References

Alavi M (1994) Tectonics of the Zagros orogenic belt of Iran: New data and interpretations, *Tectonophysics* 229: 211–238.

Allen RM, Kanamori H (2003) The potential for earthquake early warning in southern California. *Science* 300:786–789.

Allen RM (2007) The ElarmS earthquake early warning methodology and application across California. In Gasparini P., Manfredi G., Zschau J. (eds) Earthquake Early Warning Systems. *Springer*, Berlin: 21-43.

Asudeh I (1982) Seismic structure of Iran from surface and body wave data, *Geophysical Journal of the Royal Astronomical Society* 71: 715–730.

Berberian M (1976) Contribution to the seismotectonic of Iran, part II, *Geological Survey of Iran*, Report No. 39, (in Persian).

Berberian M (2014) Earthquakes and coseismic surface faulting on the Iranian Plateau. A historical, social, and physical approach, Elsevier, *Developments in Earth Surface Processes* 17: 714 p.

BHRC (2018a) Building & Housing Research Center (BHRC) of Iran. *Iran Strong Motion Network, Waveforms*, https://smd.bhrc.ac.ir/Portal/en/Search/Waveforms. Accessed 22 October 2018.

BHRC (2018b) Building and Housing Research Center (BHRC) of Iran. *Iran Strong Motion Network, Stations*, https://smd.bhrc.ac.ir/Portal/en/Search/Stations. Accessed 22 October 2018.

Boore DM, Atkinson GM (2008) Ground-Motion Prediction Equations for the Average Horizontal Component of PGA, PGV, and 5%-Damped PSA at Spectral Periods between 0.01 s and 10.0 s Earthquake *Spectra* 24: 99–138.

Borcherdt RD, Gibbs JF (1976) Effects of local geological conditions in the San Francisco Bay region on ground motions and the intensities of the 1906 earthquake. *Bulletin of the Seismological Society of America* 66: 467–500.

Borcherdt RD, Glassmoyer G (1992) On the characteristics of local geology and their influence on ground motions generated by the Loma Prieta earthquake in the San Francisco Bay region, California. . *Bulletin of the Seismological Society of America* 82: 603–641.

Colombelli S, Zollo A (2015) Fast determination of earthquake magnitude and fault extent from real-time P-wave recordings, *Geophysical Journal International* 202: 1158–1163.

Colombelli S, Zollo A, Festa G, Kanamori H (2012) Early magnitude and potential damage zone estimates for the great Mw 9 Tohoku-Oki earthquake, Geophysical Research Letters 39: L22306, doi:10.1029/2012GL053923.

Dehghani G, Makris J (1984) The gravity field and crustal structure of Iran, *Neues Jahrbuch für Geologie und Paläontologie Abhandlungen* 168: 215-229.

Delouis B, Charlety J, Vallee M (2009) A Method for Rapid Determination of Moment Magnitude Mw for Moderate to Large Earthquakes from the Near-Field Spectra of Strong-Motion Records (MWSYNTH), *Bulletin of the Seismological Society* 99:1827–1840.

Douglas J (2019) Ground motion prediction equations 1964–2018, http://www.gmpe.org.uk/gmpereport2014.pdf, Accessed 20 May 2020.

Engdahl ER, Bergman EA, Myers SC (2008) Seismotectonics of the Iran Region, *American*

Geophysical Union, Fall Meeting 2008, abstract No. T23D-06.

Engdahl ER, Jackson JA, Myers SC, Bergman EA, Priestley K (2006) Relocation and assessment of seismicity in the Iran region, *Geophysical Journal International* 167: 761–778.

Eurocode 8 (2004) Design of structuresfor earthquake resistance – Part 1: General rules, seismicactions and rules for buildings, *The European Standard EN* 1998-1:2004.

Festa G, Zollo A, Lancieri M (2008) Earthquake magnitude estimation from early radiated energy, *Geophysical Research Letters* 35: L22307, doi:10.1029/2008GL035576.

Ghodrati GA, Mahdavian A, Manouchehri F (2007) Attenuation Relationships for Iran, *Journal of Earthquake Engineering* 4: 469-492.

Heidari H, Shomali ZH, Ghayamghamian MR (2013) Magnitude-scaling relations using period parameters τc and τpmax, for Tehran region, Iran, *Geophysical Journal International* 192: 275–284.

Joyner WB, Boore DM (1981) Peak horizontal acceleration and velocity from strong-motion records including records from the 1979 Imperial Valley, California, earthquake, *Bulletin of the Seismological Society of America* 71: 2011–2038.

Kanamori H (1993) Locating earthquake with amplitude: Application to real-time seismology, *Bulletin of the Seismological Society of America* 83: 264-268.

Kanamori H, Hauksson E, Heaton T (1997) Real-time seismology and earthquake hazard mitigation, *Nature* 390: 461–464.

Lee J, Friederich W, Meier T (2012) Real time monitoring of moment magnitude by waveform inversion, *Geophysical Research Letters* 39: L02309, doi:10.1029/2011GL050210.

Lin TL, Wu YM (2012) A Fast Magnitude Estimation for the 2011 Mw 9.0 Great Tohoku Earthquake, *Seismological Research Letters* 83: 666-671.

Mase LZ, Likitlersuang S, Tobita T (2018a) Analysis of seismic ground response caused during strong earthquake in Northern Thailand, *Soil Dynamic and Earthquake Engineering* 114: 113-126.

Mase LZ, Likitlersuang S, Tobita T (2018b) Non-linear Site Response Analysis of Soil Sites in Northern Thailand during the Mw 6.8 Tarlay Earthquake, *Engineering Journal* 22: 291-303

Midorikawa S, Matsuoka M, Sakugawa K (1994) Site effects on strong-motion records observed during the 1987 Chiba-Ken-Toho-Oki, *Japan Earthquake. Proceedings of 9th Japan EarthquakeEngineering Symposium* 3: 85–90.

Nasiripour B (2006) Moho depth and crustal Vp/Vs ratio in Khorasan provinces inferred from receiver functions of teleseismic events observed by the Khorasan seismic network, MSc Thesis, *Ferdowsi University of Mashhad*, Mashhad, Iran.

Nazeri S, Shomali ZH, Colombelli S, Elia L, Zollo A (2017). Magnitude Estimation Based on Integrated Amplitude and Frequency Content of the Initial P Wave in Earthquake Early Warning Applied to Tehran, Iran, *Bulletin of the Seismological Society of America* 107: 1432-1438.

NEHRP (1997) National Earthquake Hazards Reduction Program (NEHRP). Recommended provisions for seismic regulation for new buildings and other structures edition, Part 1: *Provisions*, FEMA, Washington, DC.

Nowroozi A (1976) Seismotectonic provinces of Iran, *Bulletin of the Seismological Society of America* 66: 1249–1276.

Pankow KL, Pechmann JC (2004) The SEA99 ground-motion predictive relations for extensional tectonic regimes: Revisions and a new peak ground velocity relation, *Bulletin of the Seismological Society of America* 94: 341–348.

R Core Team (2020). R: A language and environment for statistical computing. Vienna, Austria, https://www.R-project.org/, Accessed 20 May 2020.

Sadeghi-Bagherabadi A, Sadeghi H, Fatemi Aghda SM, Sinaeian F, Mirzaei-Alavijeh H, Farzanegan E, Hosseini SK, Babaei P (2013) Real-Time Mapping of PGA Distribution in Tehran Using TRRNet and peeqMap, *Seismological Research Letters* 84: 1004-1013.

Saffari H, Kuwata Y, Mahdavian A (2017) Site amplification of Iran's major Seismic zones using attenuation relationship, *Journal of Earthquake Engineering* doi:10.1080/13632469.2017.1323045.

Shahbazi P, Mansouri B (2019) Loss Modeling for 2017 Sarpol-e Zahab Earthquak, *Journal of Seismology and Earthquake Engineering* 20: 69-80.

Standard 2800, 2014. Iranian code of practice for seismic resistant design of buildings, 4th edn, *BHRC Publication*, Tehran, Iran.

Takin M (1972) Iranian geology and continental drift in the Middle East, *Nature* 235: 147–150.

USGS (2020), Where do earthquakes occur? https://www.usgs.gov/faqs/, Accessed 20 May 2020.

Walker R, Jackson J (2004) Active tectonics and late Cenozoic strain distribution in central and eastern Iran, *Tectonics* 23: TC5010.

Wessel P, Smith WHF (1998) New improved version of Generic Mapping Tools released. EOS Trans. *American Geophysical Union* 79: 579-579.

Weisberg S (1980) Applied linear regression, *Wiley*, New York.

Wu YM, Kanamori H (2008) Exploring the feasibility of on-site earthquake early warning using close-in records of the 2007 Noto Hanto earthquake, *Earth Planets and Space* 60: 155–160.

Wu YM, Teng TL (2004) Near real-time magnitude determination for large crustal earthquakes, *Tectonophysics* 390: 205-216.

Zaarour N, Melachrinoudis E (2019) What's in a Coefficient? The "Not so Simple" Interpretation of R 2, for Relatively Small Sample Sizes, *Journal of Education and Training Studies* 7: 27-40.

Zare M, Brad PY, Ghafory-Ashtiany M (1999) Site characterizations for the Iranian strong motion network, *Soil Dynamics and Earthquake Engineering* 18: 101-123.

Zollo A, Amoroso O, Lancieri M, Wu YM, Kanamori H (2010) A threshold-based earthquake early warning using dense accelerometer networks, *Geophysical Journal International* 183: 963–974.